

Figure 1. Gated-SPECT description. RR interval is divided into equally spaced temporal phases. A full volume dataset is obtained for each temporal phase.

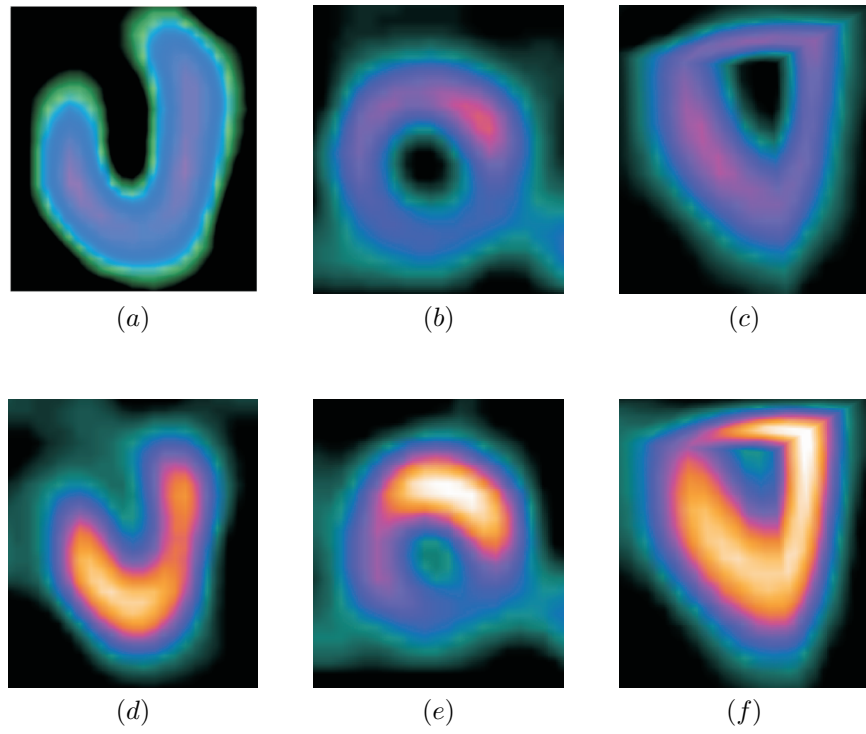


Figure 2. Example of gated-SPECT study. (a) Long axis, (b) short axis and (c) 3D views at End-diastole. (d) Long axis, (e) short axis and (f) 3D views at End-systole.

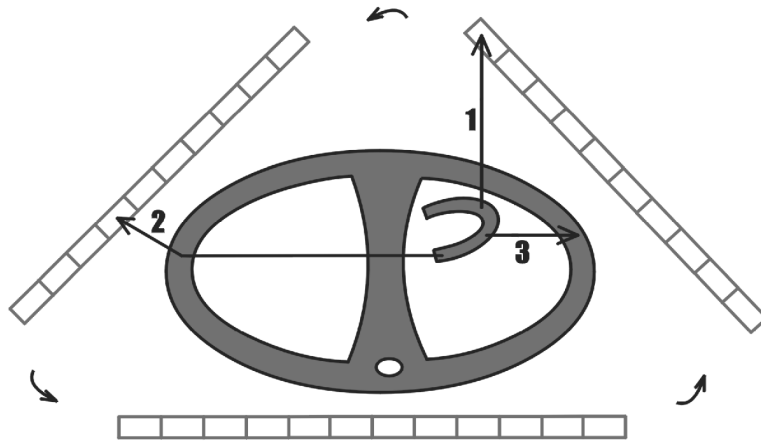


Figure 3. Three kinds of photons are present during image construction: (1) fully contributing photons, (2) scattered Photons, and (3) completely absorbed photons.

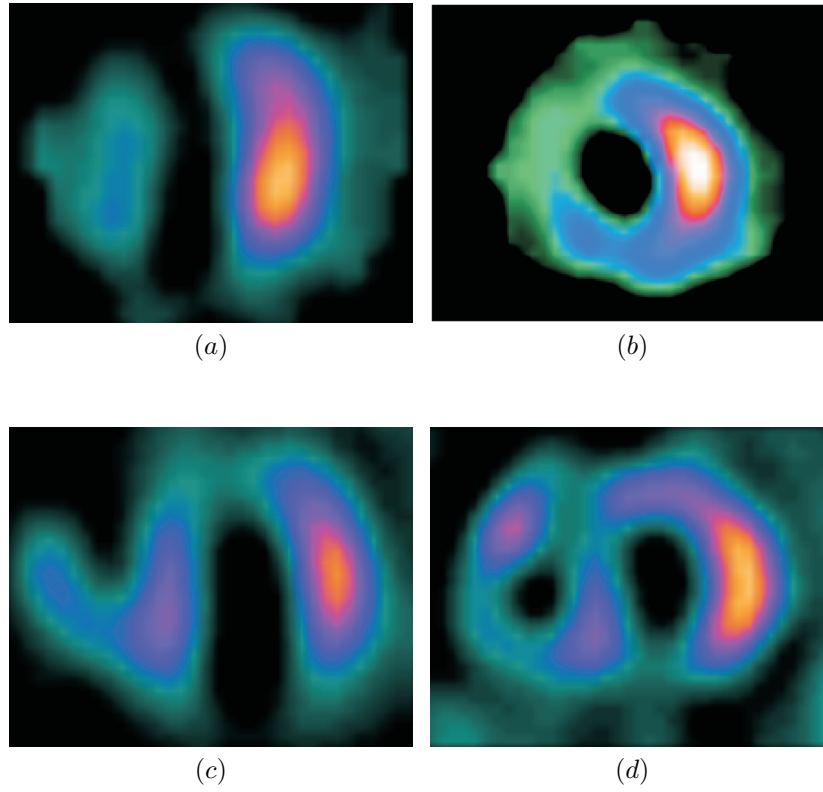


Figure 4. Some of the challenges inherent to gated-SPECT imaging: perfusion defects. (a)–(c) Long axis and (b)–(d) short axis views.

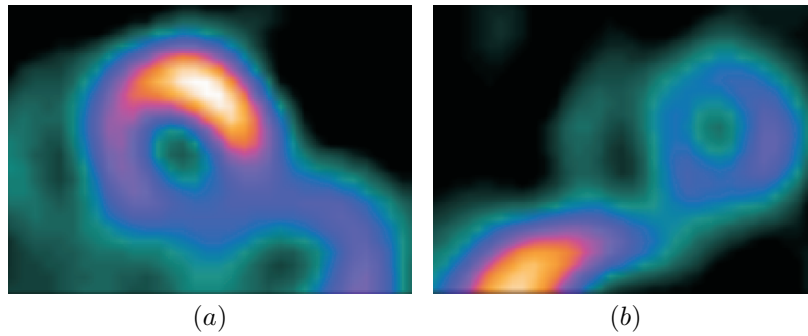


Figure 5. Some of the challenges inherent to gated-SPECT imaging: extra cardiac uptake. (a) Bowel uptake that does not affect activity counts. (b) Liver uptake that affects normalization of activity counts.

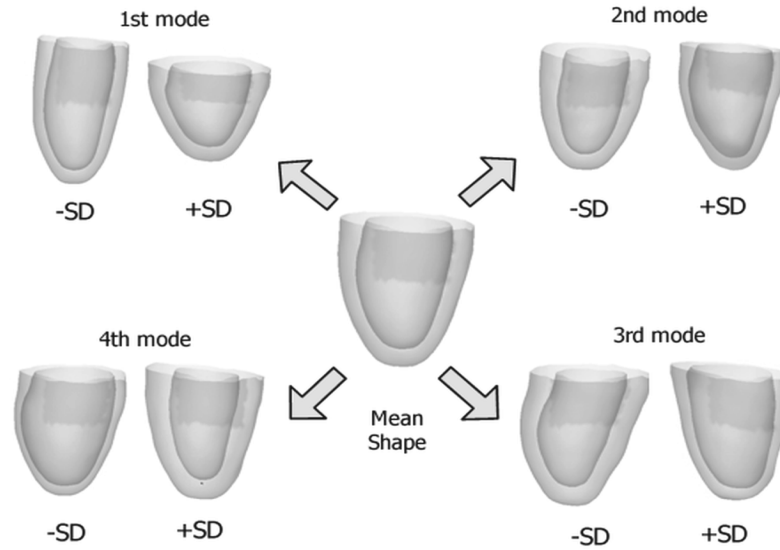


Figure 6. Principal modes of variation for the MRI (ED) PDM. The shapes are generated by varying a single model parameter, (b_i) , fixing all others at zero standard deviations ($SD_i = \sqrt{\lambda_i}$) from the mean shape.

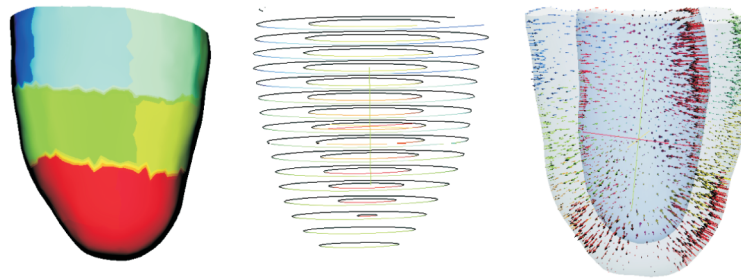


Figure 7. Convergence of the algorithm. Initialization (left), intermediate step (center), and convergence (right).

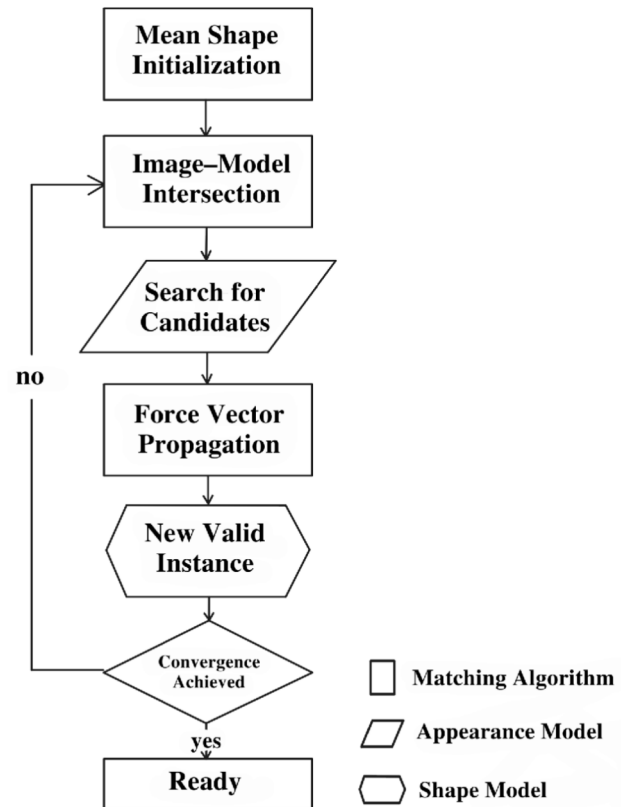


Figure 8. 3D-ASM matching procedure flowchart.

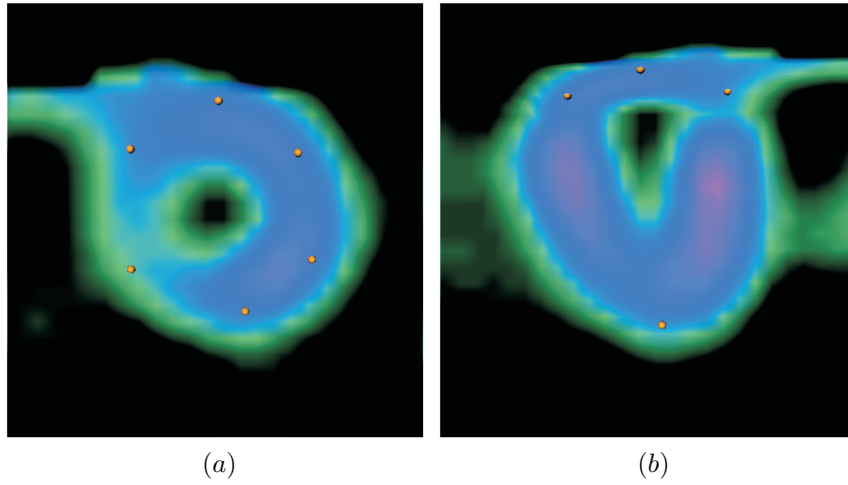


Figure 9. Initialization points: (a) SA and (b) biplane views.

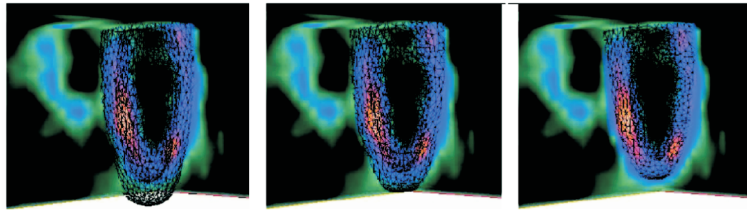


Figure 10. Convergence of the algorithm. Initialization (left), intermediate step (center), and convergence (right).

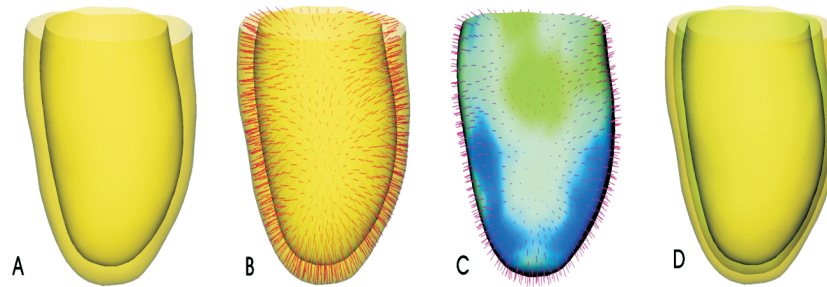


Figure 11. Central surface calculation. For every point in the endocardial surface, the shortest distance to the epicardial surface is assessed. The middle points in all these segments are collected and based on the same mesh connectivity of the endocardial surface; a new mesh is built. (a) Original surface; (b–c) segment evaluation, and (d) generated central surface.

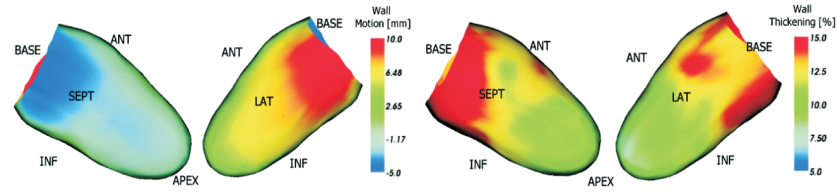


Figure 12. Left: wall motion, ED and ES, respectively. Right: wall thickening assessment, ED and ES, respectively.

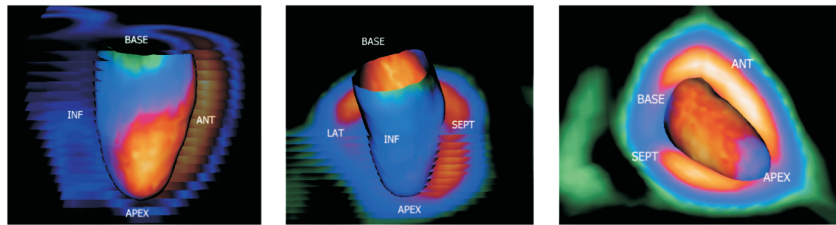


Figure 13. Perfusion map corresponding to ES displayed in different views.

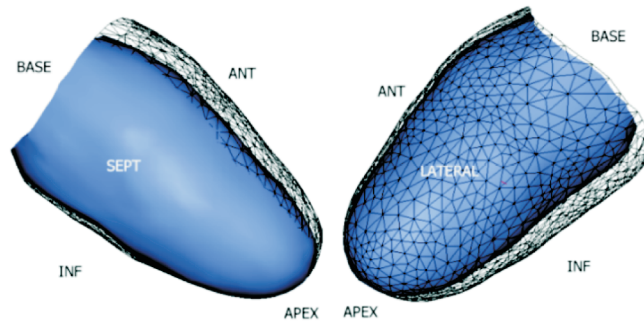


Figure 14. Endocardial Excursion.

CHAPTER 6: STATISTICAL DEFORMABLE MODELS FOR CARDIAC SEGMENTATION

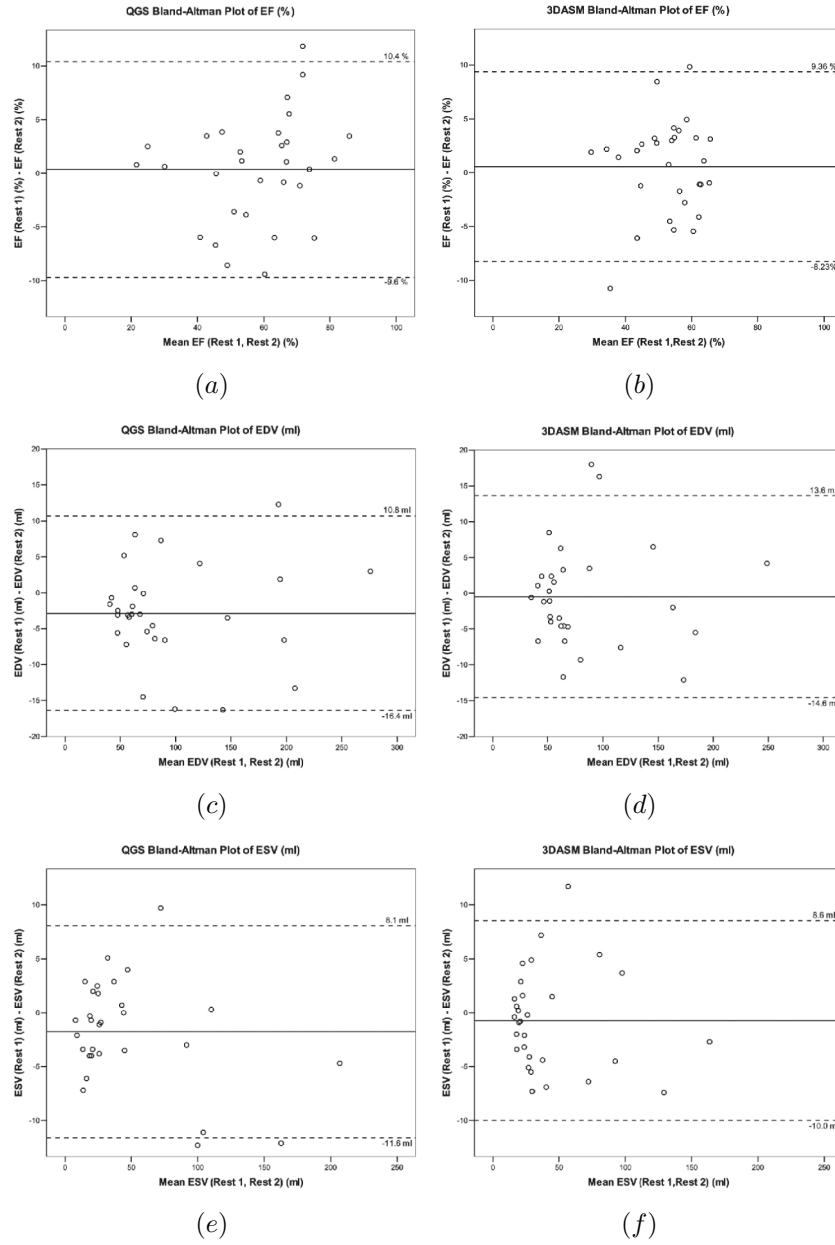


Figure 15. Bland-Altman Plots of EF (a–b), EDV (c–d), and ESV (e–f) comparing first and second rest studies estimated with QGS (left) and 3DASM (right).

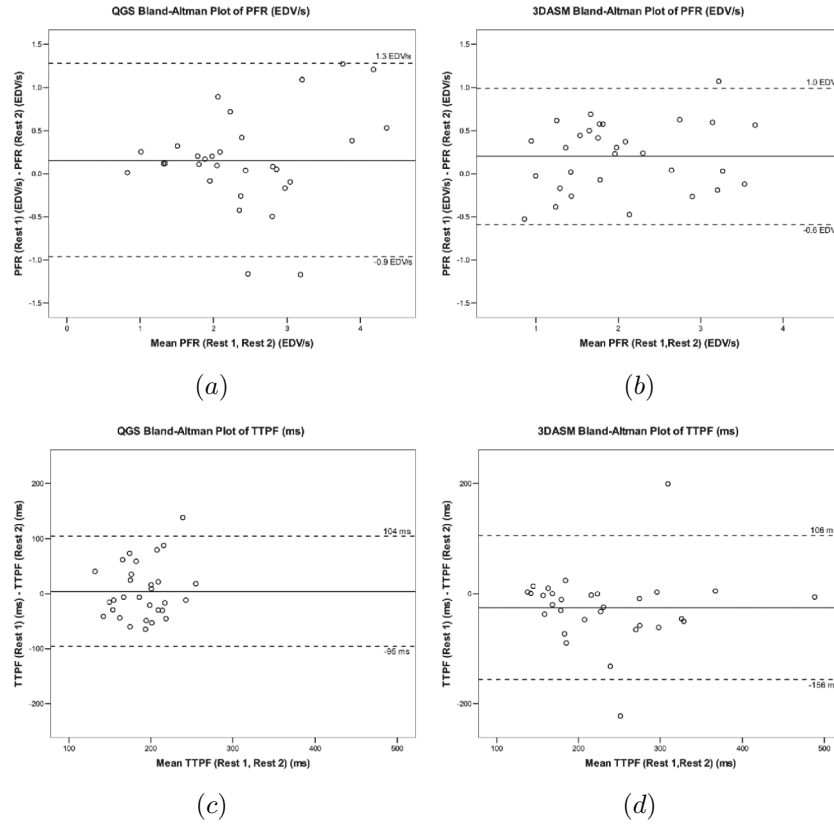


Figure 16. Bland-Altman Plots of PFR (a–b) and TTPF (c–d) comparing first and second rest studies estimated with QGS (left) and 3DASM (right).

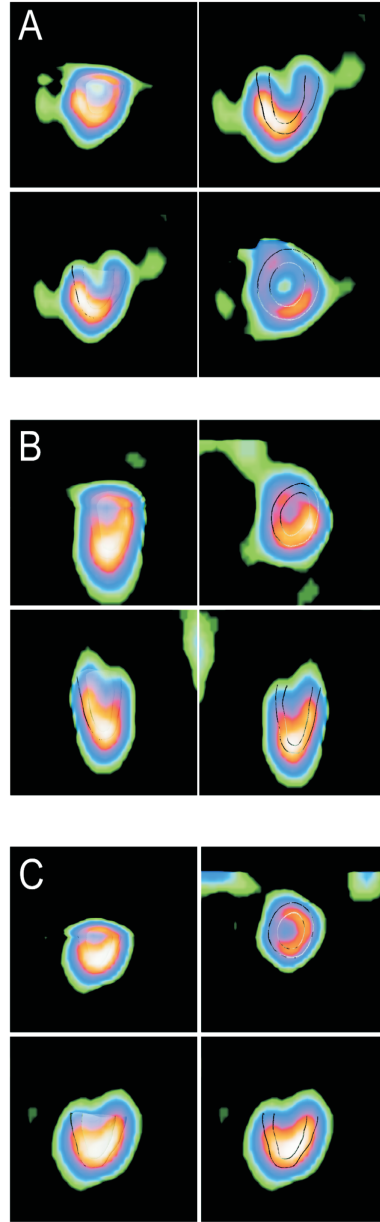


Figure 17. (a–c) Some examples of end systole segmentation results obtained with 3DASM of cases with the greatest difference on EF calculations.

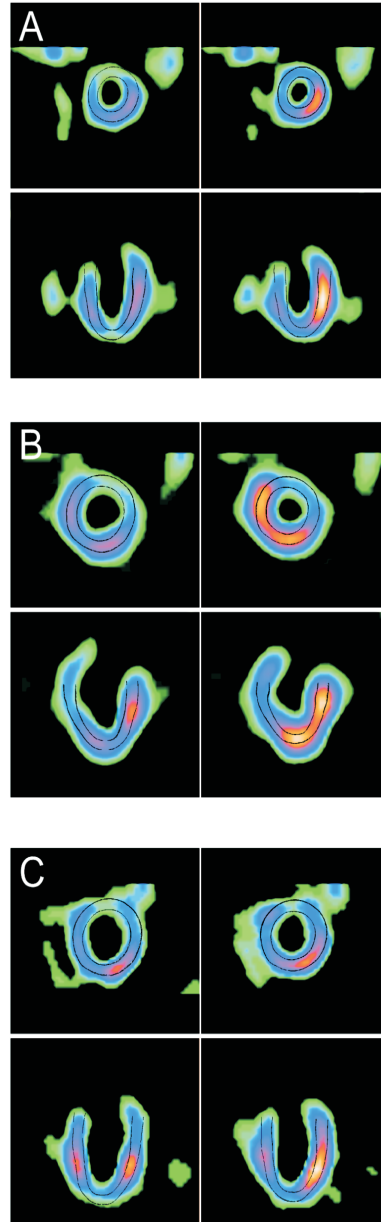


Figure 18. (a–c) Segmentation results obtained with 3DASM of cases with the greatest difference on EDV calculations. ED segmentation results are displayed on the left and ES results on the right.

CHAPTER 6: STATISTICAL DEFORMABLE MODELS FOR CARDIAC SEGMENTATION

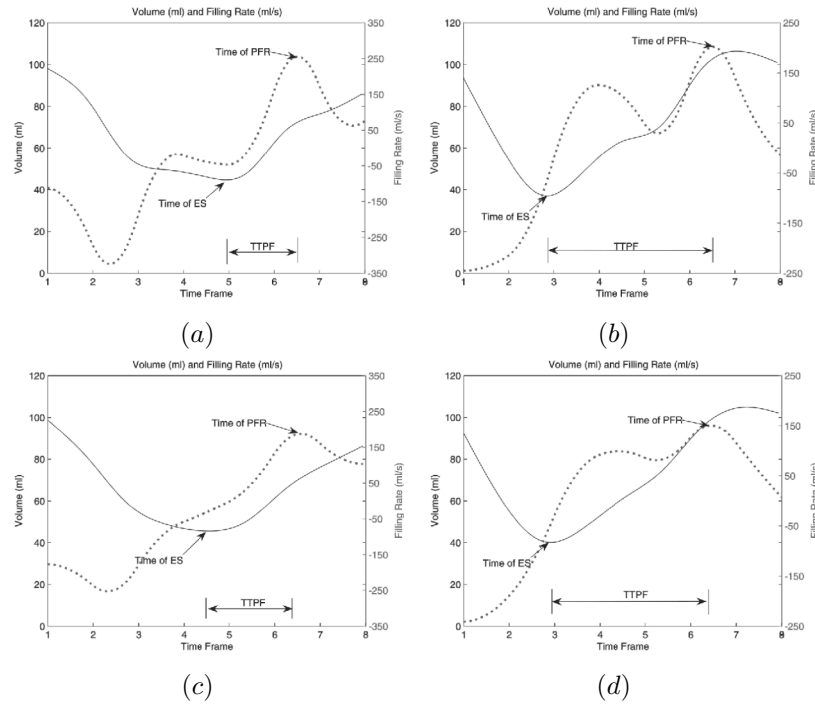


Figure 19. Volume and filling rate curves with different interpolation techniques. (a–b) Top row shows restrictive interpolation results and (c–d) bottom row displays smooth curves. **Left:** both plots (a–c) were obtained with data from the same patient. **Right:** both plots (b–d) were obtained with data from the same patient. Notice the difference in time of ES and PFR, length of TTPF (arrow), amplitude, and shape.